JOURNAL OF MECHANICAL ENGINEERING, SCIENCE, AND INNOVATION
ITATS
Research Article

Numerical study the effect of inlet and outlet ventilation configurations for passive cooling air conditioning system

Journal of Mechanical Engineering, Science, and Innovation
e-ISSN: 2776-3536
2024, Vol. 4, No. 2
DOI: 10.31284/j.jmesi.2024.v4i2.6659
ejurnal.itats.ac.id/jmesi

Arrad Ghani Safitra[1*], Lohdy Diana[1], Joke Pratilastiarso[1], Nur Hidayat[1]

[1]Politeknik Elektronika Negeri Surabaya, Indonesia

Corresponding author:
Arrad Ghani Safitra
Politeknik Elektronika Negeri Surabaya
Email: arradgs@pens.ac.id

Abstract

The application of green energy technology through passive cooling systems offers a solution to achieve energy savings and reduce CO_2 emissions. This study focuses on the simulation of room conditions using the computational fluid method with the aims of determining the effect of inlet and outlet configuration against the air condition in the room. There are 3 variations to evaluate the distribution of air temperature, air humidity, and air velocity, the variation are: Variation 1: two inlets – one outlet, Variation 2: two inlets – two outlets, Variation 3: four inlets – three outlets. The simulation used k-epsilon as a turbulent model, SIMPLE algorithm, and second order for discretization. The results presented in this simulation are the distribution of air temperature, air humidity, and air velocity. The results of the study show Variation 3 has the best design if cooling or heating equipment wants to be added, for example passive cooling in summer and a heater for cold weather. On other hand, Variation 1 is the most effective in maintaining the stability of humidity distribution and air velocity within the room. This configuration successfully creates optimal ventilation by generating efficient natural convection without significant fluctuations, achieved using two inlets and one active outlet.

Keywords: *Energy, passive cooling, cooling process, temperature.*

Received: September 29, 2024; Received in revised: November 28, 2024; Accepted: November 30, 2024
Handling Editor: Ika Nurjannah

INTRODUCTION

In general, climate change is becoming increasingly perceptible, significantly impacting indoor air conditions in buildings where people carry out daily activities. The

building sector and the activities within buildings account for about 32-48% of global energy demand, with the primary energy consumption allocated to conventional HVAC (Heating, Ventilation, and Air-Conditioning) systems [1-4]. This demand will continue to increase, given that more than 50% of new buildings in Asia are constructed each year. The International Energy Agency predicts that electricity demand for cooling will reach 37% from 2016 levels and will continue to grow until 2050 [5]. The comfort level suitable for a particular room is determined using Psychometrics. Through psychometrics, the appropriate equipment can be selected to avoid disturbing human comfort [6]. Research has varied the input and output air configurations in a greenhouse building. These configurations include Natural Ventilation; Naturally Ventilated & Buried & Shaded Greenhouse; Naturally Ventilated & Buried Greenhouse; Naturally Ventilated & Shaded Greenhouse; Naturally Ventilated Greenhouse. The research results show that Naturally Ventilated & Buried & Shaded Greenhouse can produce the highest savings among the variations [7]. Water is generally used as a cooling medium due to the following factors: 1. Water is a material that is readily available in large quantities. 2. It is easy to manage and process. 3. It absorbs relatively high heat per unit volume. However, this study compares water and glycol as cooling media. The results show that glycol cools the CPU surface faster than water [8]. A parametric study of the overall flow regime was conducted to describe the impact of the relevant parameters on velocity, temperature, skin friction coefficient, and local Nusselt number. It is evident that CuO-EG nanofluids cause a rapid decrease in temperature within the boundary layer [9]. The experiment studies the cooling performance of freshwater and seawater for evaporative air cooling. The study demonstrates the feasibility of evaporative cooling using seawater, which is a significant benefit for evaporative cooling applied in coastal areas to conserve freshwater [10]. The characteristic of spray-type liquid coolers is that the non-corrosive cooling liquid is sprayed directly onto the surface of the thermal element or the expansion surface in contact with the thermal element. After absorbing heat, the thermal fluid is discharged [11].

Apart from experiments, simulation methods are needed before carrying out design. It is called The Computational Fluid Dynamics (CFD). It can reduce testing costs. CFD is a part of fluid mechanics that uses numerical analysis and algorithms to solve and analyze problems involving fluid flows. By applying computational methods to the governing equations of fluid dynamics, such as the Navier-Stokes equations, CFD allows for the simulation of complex fluid behaviors in various systems. This includes predicting the movement and interaction of fluids, heat transfer, and chemical reactions within a virtual environment. The process typically involves creating a digital model of the physical system, discretizing the domain into a mesh of smaller elements, solving the equations for each element, and then analyzing the results to understand and optimize fluid behavior. Several simulations have been carried out to determine the air condition in the room. Air conditioning simulation studies have been widely conducted to understand air characteristics such as air temperature distribution and airflow direction [12-19]. For instance, this research simulates airflow patterns in contact with the human body. The results show differences in airflow patterns and distribution of contaminant when realistic walking motion is applied to the model of human, compared to simplified models of motion. Contaminant leakage from the All room ranges from 20.6% to 28.6%, indicating that previous studies may have underestimated infection risks due to overly simplified human models and motions. These results underscore the importance of applying realistic human models and movements in CFD simulations for accurate infection risk assessment in spaces. [20]. A simulation of airflow in an underfloor air distribution (UFAD) system using Computational Fluid Dynamics (CFD) methods showed that finer mesh sizes produced more accurate simulations, although requiring longer computation

times [21]. Another study analyzed temperature distribution and airflow in naturally ventilated rooms during winter, showing that CFD simulations are effective in designing ventilation to improve thermal comfort, though there was a slight overestimation of temperature [22]. Another study utilized CFD simulations to optimize HVAC systems by modeling airflow to enhance thermal comfort. The location of air supply devices was found to significantly affect comfort, and the CFD-based approach proved more effective in evaluating indoor climate control strategies compared to traditional methods [23]. The final study examined the impact of different types of natural ventilation on the thermal environment, with jalousie windows proving more effective in improving air quality and thermal comfort than top-hang windows [24].

Building on the issues outlined, this research focuses on simulating indoor room conditions using computational fluid dynamics (CFD). The primary objective is to analyze the effects of various inlet and outlet ventilation configurations on a passive cooling air-conditioning system. The simulation evaluates air temperature, humidity, and velocity distributions under three distinct inlet-outlet configurations. It is conducted in three dimensions for comprehensive airflow analysis.

METHODS

This research used Computational Fluid Dynamics Method with Ansys Fluent Software. In the simulation approach, the process begins are drawing the geometry, followed by meshing, inputting parameter settings, running the simulation, validating results, and performing post-processing. The simulation uses 3 dimensions with geometry dimension 758 cm x 730 cm x 310 cm, the size is equated to the size of a room

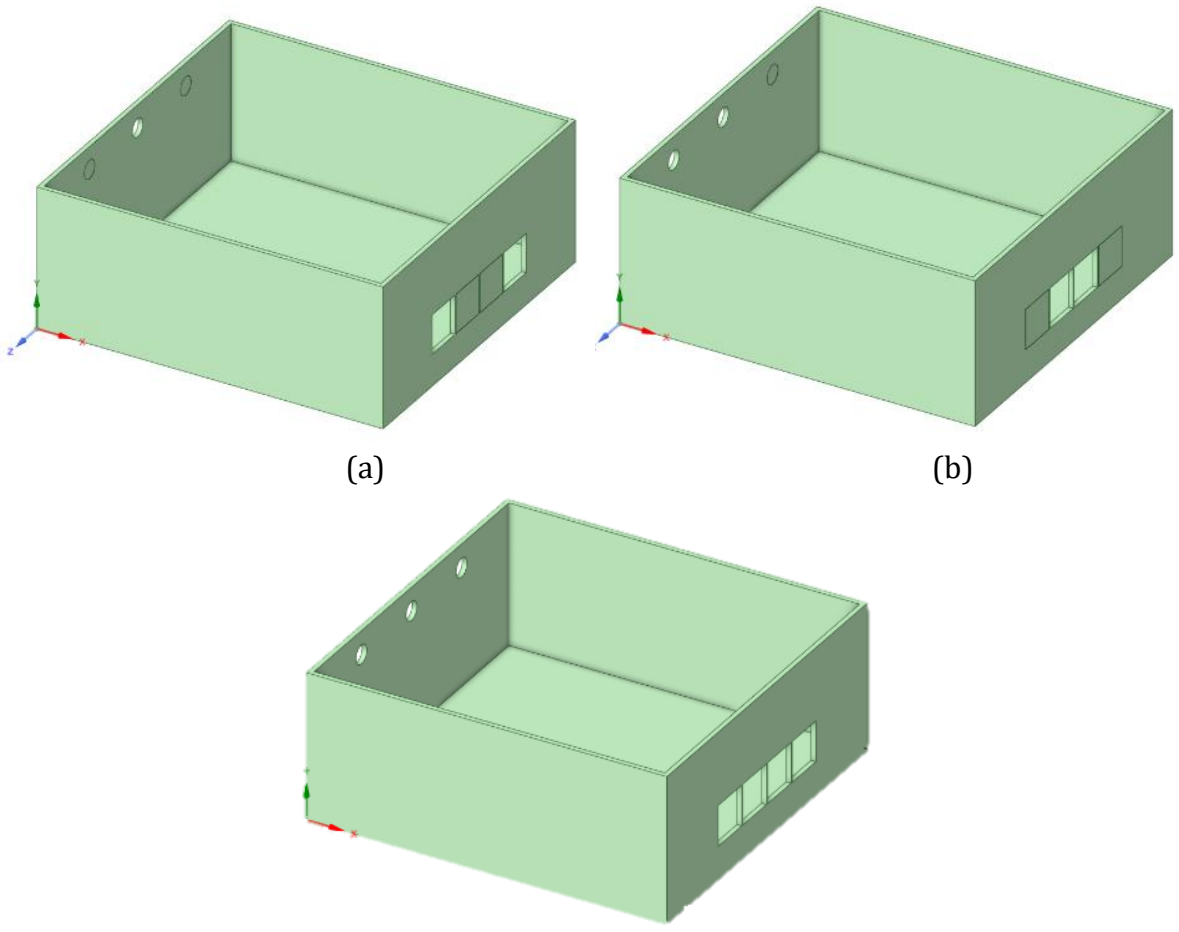

(a) (b)

(c)

Figure 1. Geometry (a) Variation 1, (b) Variation 2, and (c) Variation 3

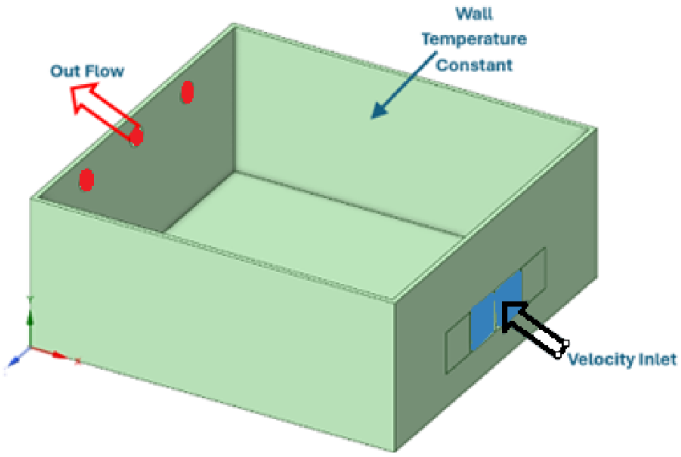

(a)

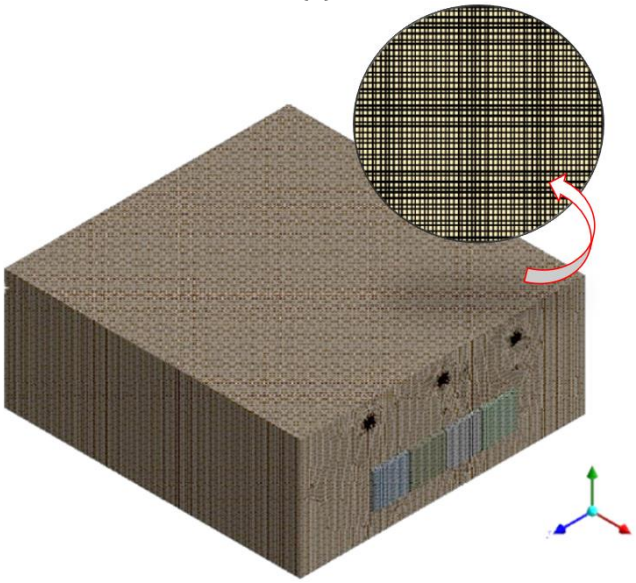

(b)

Figure 2. (a) Boundary Condition, (b) Meshing of Geometry

used for student activities. This research variation consists of three variations: Variation 1: two inlets – one outlet as can be seen in Figure 1(a), Variation 2: two inlets – two outlets as can be seen in Figure 1(b), Variation 3: four inlets – three outlets as can be seen in Figure 1(c).

The boundary condition can be seen in Figure 2 (a). Meshing in Computational Fluid Dynamics (CFD) involves dividing the model's geometry into small, discrete cells, as shown in Figure 2 (b) with 0,42 for skewness as a mesh quality parameter, it means the mesh has very good quality. The simulation used k-epsilon as a turbulent model, SIMPLE algorithm, and second order for discretization. This research utilizes Computational Fluid Dynamics (CFD) software, encompassing several key modeling steps. Initially, room geometry is drawn to create a virtual representation of space. Following this, meshing is performed to divide the geometry into discrete elements, which facilitates computational analysis. Next, the properties of the cooling fluids are inputted into the software to accurately simulate their behavior within the model as can be seen in Table 1. This simulation uses five meshes to determine the stable mesh used to analyze the results. After simulating all the meshes, the mesh used hexahedral type with 1.466.000 number of cells that has lowest error or in stable condition for outlet air temperature as can be seen in Table 2. The simulation is then run to analyze the airflow and cooling effects. Finally, data is collected, including contour maps and temperature graphs, to evaluate the performance of the cooling.

Table 1. Properties of Fluid and Wall

Properties	Value	Unit
Inlet Air Temperature	303	K
Inlet Air velocity	0.5	m/s
Air Relative Humidity	67.5	%
Air Density	1.225	kg/m^2
Air Specific Heat	1006.43	J/kg.K
Air Thermal Conductivity	0.0242	W/m.K
Air Viscosity	1.7894e-05	kg/m.s
Wall Material	Concrete	
Wall Temperature	300	K
Wall Density	2200	kg/m^2
Wall Specific Heat	840	J/kg.K
Wall Thermal Conductivity	1.4	W/m.K

Table 2. Grid Independency [Author result]

Mesh	Number of Cells	Outlet Air Temperature (K)	Error (%)
A	550.000	301.10	-
B	760.000	302.02	0.3046
C	970.000	302.11	0.0298
D	1.466.000	302.18	0.0232
E	1.800.000	302.18	0

RESULTS AND DISCUSSIONS

Simulation Analysis

Based on the simulation result, many results can be analyzed such as air temperature distribution, air relative humidity distribution, graph of air temperature, air humidity, and air velocity in many positions inside the room. The air temperature distribution can be seen in Figure 3. The inlet air temperature of 303 K is marked in orange colour, for all temperature variations the smallest difference is only 3 K. This is due to the low inlet air velocity and the small dimensions of the outlet causing the room to not circulate air properly. The air temperature in the near floor for all the variations has a higher temperature than in the middle room and in the top room that has lowest air temperature. The air temperature distribution in variation 1 shows high temperatures were distributed in two positions, this is because variation 1 has two inlets that are distance from each other. It is different from variation 2 where the high air temperature is only in one position, but the high-temperature area is wider than variation 1. This is because two inlets in variation 2 do not have a gap or distance. The different phenomena are shown in variation 3. It shows a relatively wide air temperature distribution. This is because variation 3 has more inlet and outlet sections than other variations. Variation 3 has the best design if cooling or heating equipment wants to be added, for example passive cooling in summer and a heater for cold weather. It is because variation 3 has the most extensive inlet area than other variations.

Figure 4 shows three variations show significant differences in humidity distribution and air velocity, reflecting how each variation affects the dynamics of airflow and heat distribution within the room. Variation 1 stands out as the most stable, with humidity and air velocity evenly distributed throughout the room. This indicates that Variation 1 has the most optimal configuration for generating efficient and consistent

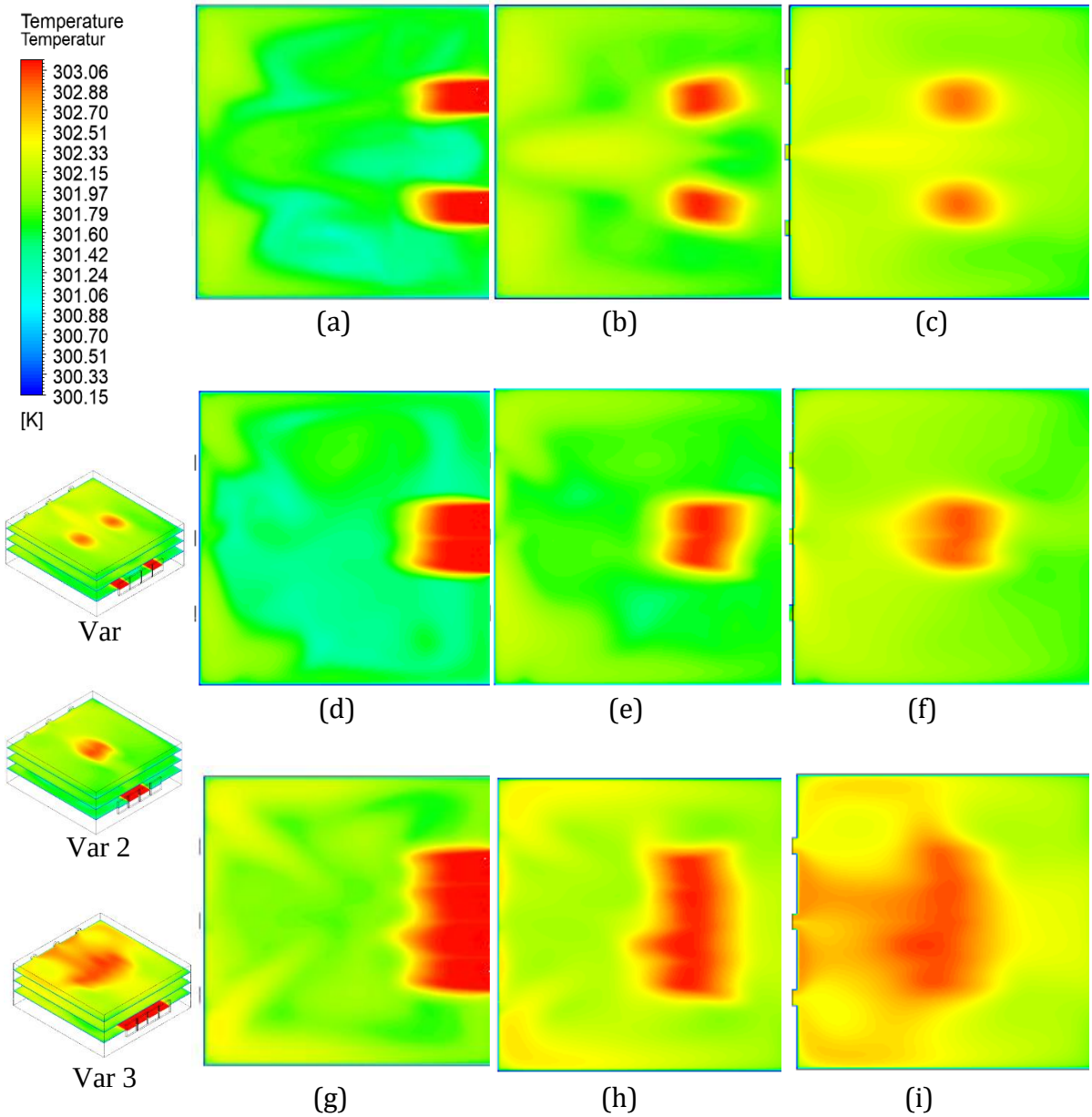

Figure 3. Distribution of Air Temperature, Variation 1 (a) near floor, (b) middle room, (c) near top, Variation 2 (d) near floor, (e) middle room, (f) near top, Variation 3 (g) near floor, (h) middle room, and (i) near top.

natural convection. This variation also demonstrates that with only two inlets and one outlet active, airflow can be managed very efficiently. Variation 2 shows stronger convection, with higher air velocity and greater humidity variations. Although it exhibits stronger convection, Variation 2 is less stable than Variation 1, due to the significant increase in velocity and larger humidity variations. This suggests that while natural convection is stronger, airflow stability is less maintained, which could cause discomfort or inefficiency in room temperature control. This could be due to the arrangement of two active inlets and two active outlets, which increase airflow dynamics but reduce stability. Variation 3 is the most unstable, with greater humidity fluctuations and lower air velocity. This indicates that Variation 3 has the least optimal arrangement, with airflow obstructions reducing the efficiency of natural convection. The less even humidity distribution and lower air velocity suggest that this variation may require adjustments in room configuration or ventilation to achieve better performance. This could be due to the activation of three inlets and three outlets, which increases airflow complexity and may

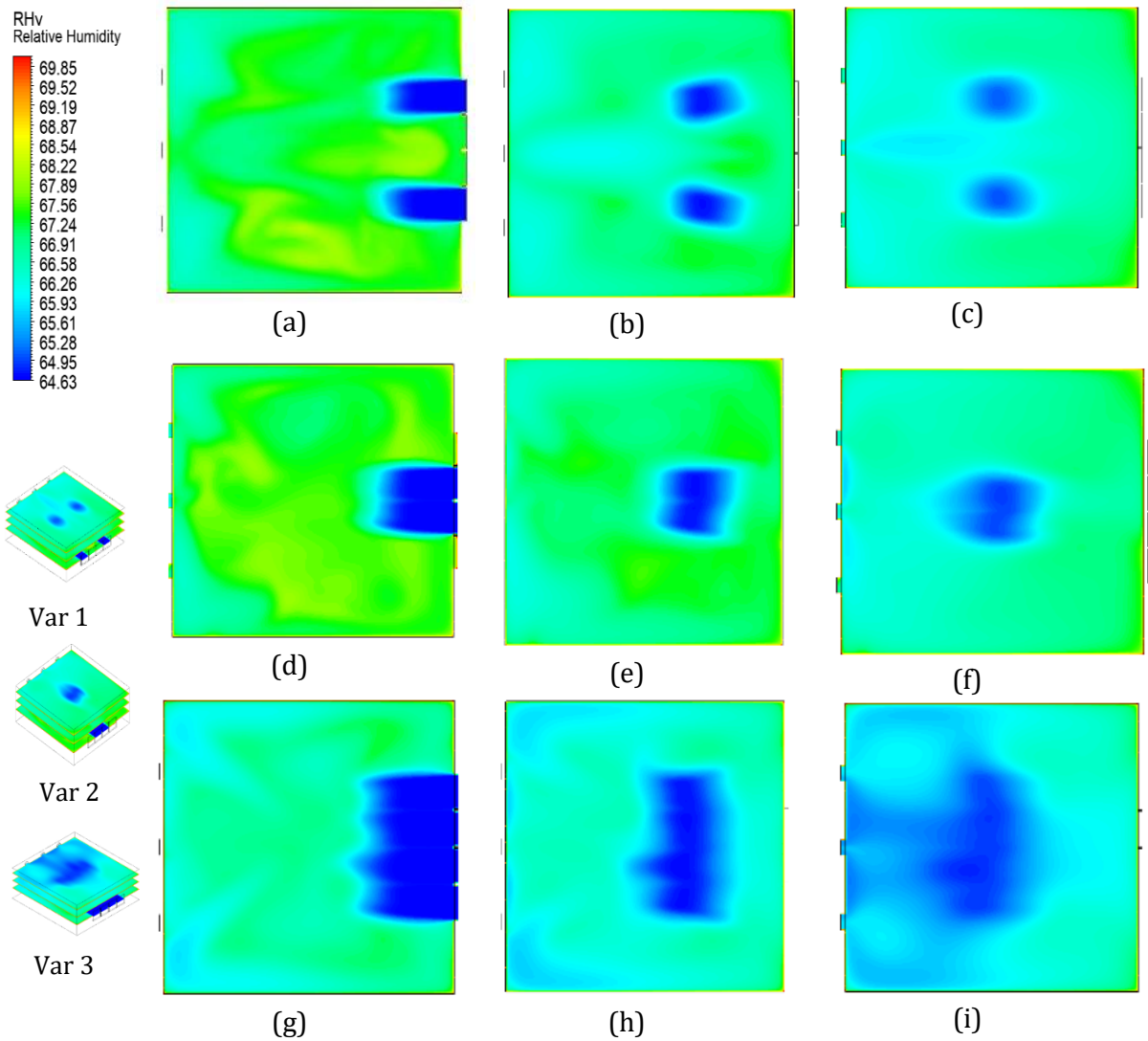

Figure 4. Distribution of Air Humidity, Variation 1 (a) near floor, (b) middle room, (c) near top, Variation 2 (d) near floor, (e) middle room, (f) near top, Variation 3 (g) near floor, (h) middle room, (i) near top.

result in higher turbulence and less even heat distribution. In conclusion, Variation 1 is the most efficient and stable in generating even and efficient natural convection. While Variation 2 has stronger convection, it needs improvement in maintaining airflow stability. Variation 3 shows a significant need for improvement in room configuration and airflow management to achieve better performance.

Figure 5 (a) illustrates the temperature distribution along Line 1, each with three variations in conditions (Variation 1, Variation 2, and Variation 3). Variation 1 shows a stable temperature trend with a slight increase from around 301.80 K at the inlet to about 302.20 K at the outlet. This indicates that natural convection along Line 1 in Variation 1 is quite uniform without significant heat accumulation. Variation 2, on the other hand, shows a sharper increase in temperature, reaching around 302.60 K at a position of approximately 2-3 meters, then slightly decreasing towards the outlet. This suggests a higher concentration of heat at certain points, possibly due to room geometry or the influence of airflow distribution. Meanwhile, Variation 3 exhibits the most significant temperature increase, reaching around 303.00 K at the 3-meter mark before gradually decreasing to around 302.40 K at the outlet, indicating strong heat accumulation at certain positions likely caused by obstructions in natural airflow.

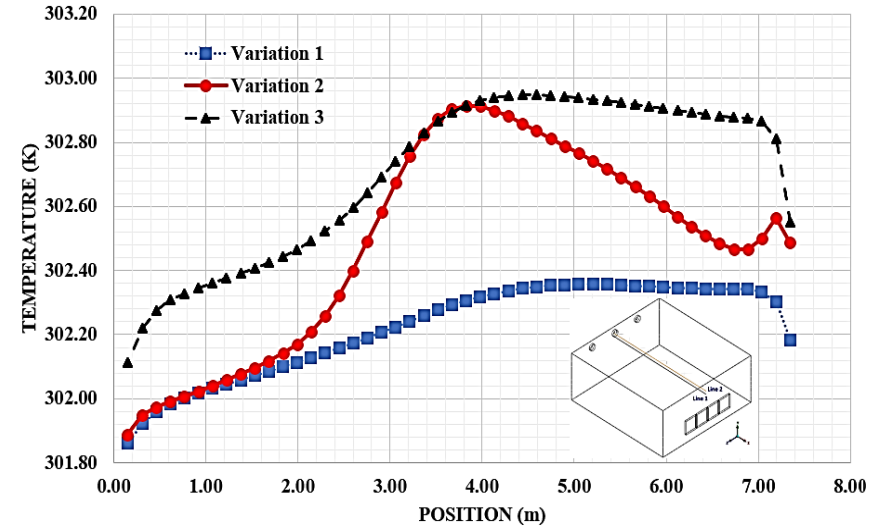

(a)

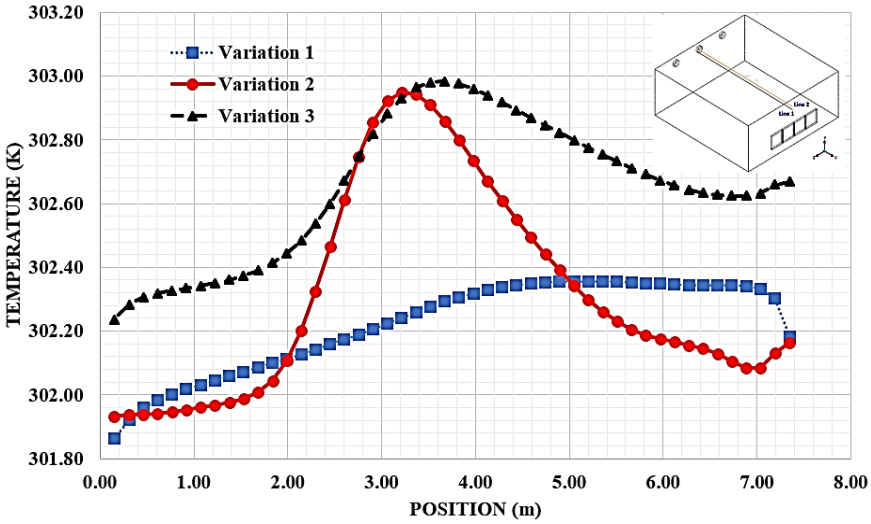

(b)

Figure 5. Air Temperature in The Middle Line (a) Line 1, (b) Line 2.

Figure 5 (b) displays the temperature distribution along Line 2. Variation 1 again shows a stable temperature trend with a slight increase from 301.80 K to 302.20 K, indicating a uniform airflow distribution without significant heat accumulation along Line 2 in Variation 1. In contrast, Variation 2 experiences a more significant temperature increase compared to Line 1, reaching around 302.70 K at the 2–3-meter mark before dropping back to around 302.30 K near the outlet. This suggests heat accumulation in the middle of Line 2, which then dissipates as it approaches the outlet. Variation 3 follows a similar pattern to Line 1, with a peak temperature reaching around 303.00 K at the 3–4-meter mark, then decreasing to around 302.60 K near the outlet, indicating substantial heat accumulation at specific points, possibly due to changes in airflow or the position of heat sources.

In each humidity distribution graph obtained from the numerical study of natural convection in a room, various trends reflect differences in humidity distribution across the three variations and the three different measurement lines. (Line 1, and Line 2) can be seen in Figure 6. Figure 6 (a) shows the humidity distribution on Line 1. Variation 1 displays a relatively stable downward trend from around 66.5% at the inlet to about 66% at around 3 meters. After that, the humidity gradually increases again towards the outlet. Variation 2 exhibits a sharper decline, starting from 66.5% at the inlet and reaching a low point of around 65.5% at the 4-meter mark before rising again towards the outlet. In each

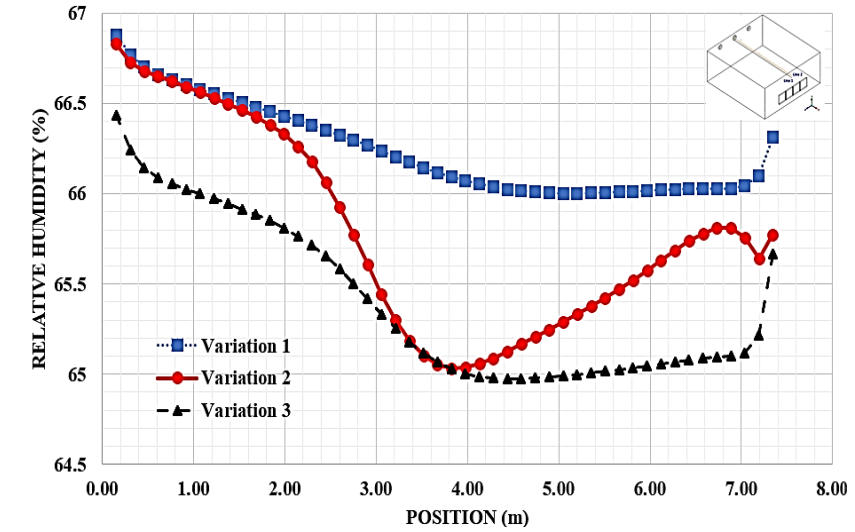

(a)

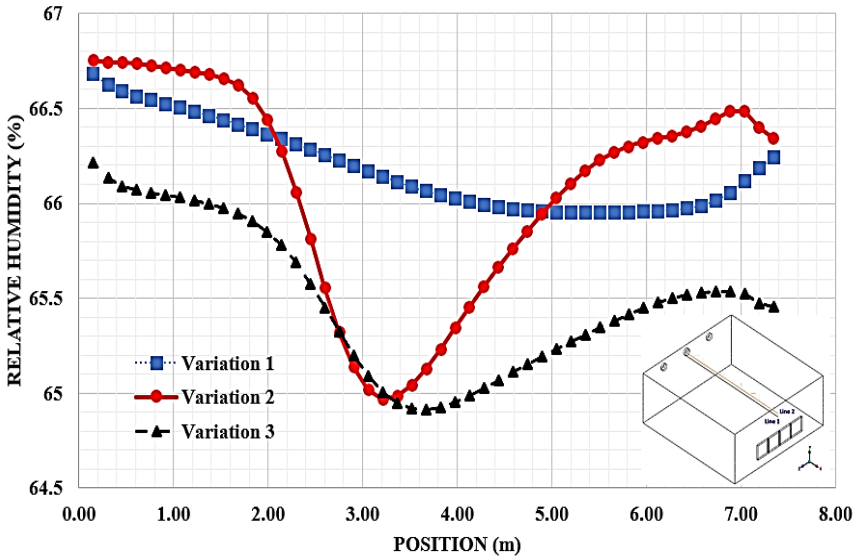

(b)

Figure 6. Air Humidity in The Middle Line (a) Line 1, (b) Line 2.

humidity distribution graph obtained from the numerical study of natural convection in a room, various trends reflect differences in humidity distribution across the three variations and the three different measurement lines. (Line 1, and Line 2) can be seen in Figure 6. Figure 6 (a) shows the humidity distribution on Line 1. Variation 1 displays a relatively stable downward trend from around 66.5% at the inlet to about 66% at around 3 meters. After that, the humidity gradually increases again towards the outlet. Variation 2 exhibits a sharper decline, starting from 66.5% at the inlet and reaching a low point of around 65.5% at the 4-meter mark before rising again towards the outlet. Variation 3 starts at 66%, drops to near 65% at the 3-meter mark, and then gradually increases to around 65.8% near the outlet. The maximum and minimum values for Variation 1 are 66.5% and 66%, for Variation 2 are 66.5% and 65.5%, and for Variation 3 are 66% and 65%. Among the three variations, Variation 1 has the highest humidity throughout the graph, while Variation 3 shows the lowest humidity levels. This suggests that Variation 1 might have a more stable and uniform airflow, while Variation 3 could be experiencing greater temperature variations or turbulence.

Figure 6 (b) shows the humidity distribution on Line 2. Variation 1 again demonstrates stability, with a very smooth downward trend from 66.5% at the inlet to around 66% at the outlet. Variation 2 shows a significant drop from 66.5% at the inlet to

65% at the 4-meter mark, followed by a rise towards the outlet. Variation 3 has a pattern similar to Variation 2, starting from 66%, dropping to 65% around the 3-meter mark, and then slightly increasing towards the outlet. The maximum and minimum values in this graph for Variation 1 are 66.5% and 66%, for Variation 2 are 66.5% and 65%, and for Variation 3 are 66% and 65%. As with Line 1, Variation 1 continues to show the highest humidity values, while Variation 3 shows the lowest, reinforcing the idea that Variation 1 has a more uniform and stable humidity distribution.

Figure 7 shows the velocity distribution graphs along the two different lines (Line 1, and Line 2) show a significant increase in speed as they approach the outlet in all three variations tested (Variation 1, Variation 2, and Variation 3). Figure 7 presents the velocity distribution on Line 1, where all variations exhibit relatively low and stable speeds from the inlet position up to around 6.5 meters, before experiencing a sharp increase near the outlet at around 7 meters. Variation 1 shows the most significant spike in speed, reaching a maximum of approximately 3.8 m/s. Variation 2 follows with a maximum of about 2.8 m/s, while Variation 3 has the smallest spike with a maximum of around 1.8 m/s. Figure 7 displays the velocity distribution on Line 2. This graph follows a similar pattern to Line 1, but the increase in speed begins earlier, around the 6-meter mark. Variation 1 shows the sharpest spike, with a maximum speed reaching around 7.8 m/s, higher than on Line 1. Variations 2 and 3 follow a similar pattern, with maximum speeds of around 6.8 m/s

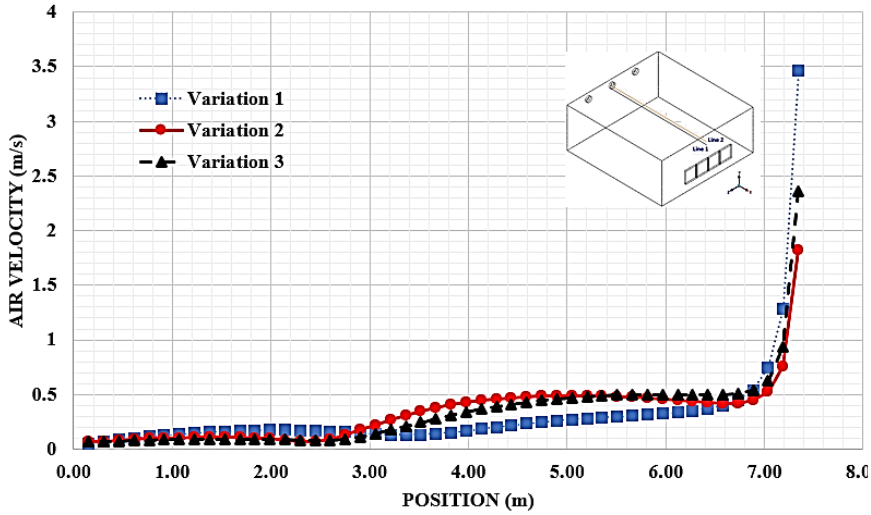

(a)

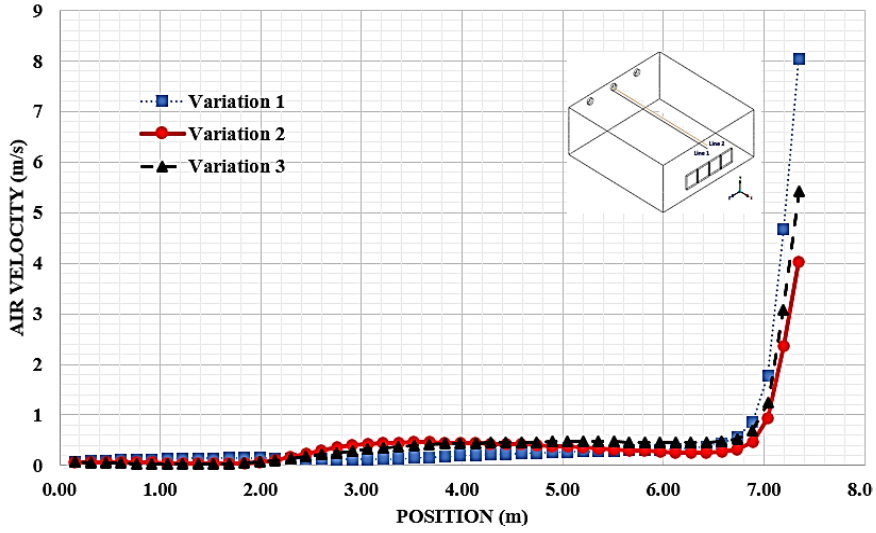

(b)

Figure 7. Air Velocity in The Middle Line (a) Line 1, (b) Line 2.

and 5.8 m/s, respectively. This indicates that Line 2, possibly due to its location within the room, has stronger natural convection compared to Line 1.

CONCLUSIONS

Based on the results of the numerical study conducted, it can be concluded that variation 3 has the best design if cooling or heating equipment wants to be added for example passive cooling in summer and a heater for cold weather, among the three variations of passive cooling system configurations tested, Variation 1 is the most effective in maintaining the stability of humidity distribution and air velocity within the room. This configuration successfully creates optimal ventilation by generating efficient natural convection without significant fluctuations, achieved using two inlets and one active outlet. In contrast, Variations 2 and 3 exhibit deficiencies in natural convection stability; although Variation 2 generates stronger convection, its low stability can lead to thermal discomfort and inefficiencies in temperature control, while Variation 3 shows uneven humidity and air velocity distribution due to suboptimal room configuration. Therefore, it is recommended to adopt a configuration similar to Variation 1 to ensure stable and efficient airflow, while Variations 2 and 3 require further improvements. This study provides a deep understanding of how passive cooling strategies can effectively reduce heat loads and support energy independence.

ACKNOWLEDGEMENTS

The author(s) would like to express their gratitude to Politeknik Elektronika Negeri Surabaya for their support during the research process. Special thanks to our research team for their contributions

DECLARATION OF CONFLICTING INTERESTS

The author(s) declared no potential conflicts of interest with respect to the research, authorship, and/or publication of this article for our colleagues

FUNDING

Appreciation to Politeknik Elektronika Negeri Surabaya for the local funding research scheme.

REFERENCES

[1] D. Ürge-Vorsatz, L. F. Cabeza, S. Serrano, and C. Barreneche, “Heating and cooling energy trends and drivers in buildings,” *Renew. Sustain. Energy Rev.*, vol. 41, pp. 85–98, 2015.

[2] I. Inayati, F. X. N. Soelami, and R. Triyogo, “Identification of existing office buildings potential to become green buildings in energy efficiency aspect,” *Procedia Eng.*, vol. 170, pp. 320–324, 2017.

[3] X. Lu, P. Xu, H. Wang, *et al.*, “Cooling potential and applications prospects of passive radiative cooling in buildings: The current state-of-the-art,” *Renew. Sustain. Energy Rev.*, vol. 65, pp. 1079–1097, 2016.

[4] A. M. Omer, “Energy, environment and sustainable development,” *Solar Thermal Engineering Journal*, vol. 12, pp. 2265–2300, 2008.

[5] International Energy Agency, “Energy Efficiency: Cooling,” [Online]. Available: https://www.iea.org/topics/energyefficiency/buildings/cooling/. [Accessed: Mar. 8, 2019].

[6] K. Vadoudi, “Development of Psychrometric diagram for the energy efficiency of Air

Handling Units," *Int. J. Ventilation*, vol. 3, no. 5, p. 491, 2018.
[7] O. Abedrabboh, M. Koç, and Y. Biçer, "Sustainable food development for societies in hot arid regions: Thermoeconomic assessment of passive-cooled soil-based and hydroponic greenhouses," *J. Cleaner Prod.*, vol. 412, p. 137250, 2023, doi: 10.1016/j.jclepro.2023.137250.
[8] M. Nazari, M. Karami, and M. Ashouri, "Comparing the thermal performance of water, ethylene glycol, alumina, and CNT nanofluids in CPU cooling: Experimental study," *Exp.* Thermal *Fluid Sci.*, vol. 57, pp. 371–377, 2014, doi: 10.1016/j.expthermflusci.2014.06.003.
[9] W. N. Mutuku, "Ethylene glycol (EG)-based nanofluids as a coolant for automotive radiator," *Asia Pacific J. Comput. Eng.*, vol. 3, pp. 1–15, 2016, doi: 10.1186/s40540-016-0017-3.
[10] R. Khatri, A. P. Singh, and V. R. Khare, "Identification of Ideal Air Temperature Distribution using different location for Air Conditioner in a room integrated with EATHE–A CFD based approach," *Energy Procedia*, vol. 109, pp. 11–17, 2017, doi: 10.1016/j.desal.2017.10.025.
[11] B. Liu, "Research on Liquid Cooling Technology and its Application in Wireless Charging," *IOP Conf. Ser.: Earth Environ. Sci.*, vol. 571, no. 1, p. 012020, Nov. 2020, doi: 10.1088/1755-1315/571/1/012020.
[12] B. Pirouz, S. A. Palermo, S. N. Naghib, D. Mazzeo, M. Turco, and P. Piro, "The role of HVAC design and windows on the indoor airflow pattern and ACH," *Sustainability*, vol. 13, no. 14, Jul. 2021, doi: 10.3390/su13147931.
[13] T. Lipinski, D. Ahmad, N. Serey, and H. Jouhara, "Review of ventilation strategies to reduce the risk of disease transmission in high occupancy buildings," *Int. J. Thermofluids*, vol. 7–8, Nov. 2020, doi: 10.1016/j.ijft.2020.100045.
[14] H. Chen, Z. Feng, and S. J. Cao, "Quantitative investigations on setting parameters of air conditioning (air-supply speed and temperature) in ventilated cooling rooms," *Indoor Built Environ.*, vol. 30, no. 1, pp. 99–113, Jan. 2021, doi: 10.1177/1420326X19887776.
[15] R. Z. Homod, A. Almusaed, A. Almssad, M. K. Jaafar, M. Goodarzi, and K. S. M. Sahari, "Effect of different building envelope materials on thermal comfort and air-conditioning energy savings: A case study in Basra city, Iraq," *J. Energy Storage*, vol. 34, Feb. 2021, doi: 10.1016/j.est.2020.101975.
[16] N. R. M. Sakiyama, J. Frick, T. Bejat, and H. Garrecht, "Using CFD to evaluate natural ventilation through a 3D parametric modeling approach," *Energies*, vol. 14, no. 8, Apr. 2021, doi: 10.3390/en14082197.
[17] S. Golder, R. Narayanan, M. R. Hossain, and M. R. Islam, "Experimental and CFD investigation on the application for aerogel insulation in buildings," *Energies*, vol. 14, no. 11, Jun. 2021, doi: 10.3390/en14113310.
[18] C. Harsito and A. N. S. Permata, "Investigation of air distribution in mosque rooms with different angles of supply and inlet velocity," *Int. J. Heat Technol.*, vol. 39, no. 4, pp. 1383–1388, Aug. 2021, doi: 10.18280/ijht.390439.
[19] M. Alkhalaf, A. Ilinca, M. Y. Hayyani, and F. Martini, "Impact of Diffuser Location on Thermal Comfort Inside a Hospital Isolation Room," *Designs*, vol. 8, no. 2, p. 19, Feb. 2024, doi: 10.3390/designs8020019.
[20] S. Jo, G. Kim, and M. Sung, "A study on contaminant leakage from Airborne Infection Isolation room during medical staff entry; Implementation of walking motion on hypothetical human model in CFD simulation," *J. Build. Eng.*, 2024, doi: 10.1016/j.jobe.2024.108812.
[21] N. A. M. Zainuddin, F. Jerai, A. A. Razak, and M. F. Mohamad, "Accuracy of CFD Simulations on Indoor Air Ventilation: Application of Grid Convergence Index on

Underfloor Air Distribution (UFAD) System Design," *J. Mech. Eng.*, vol. 20, no. 3, pp. 199–222, 2023, doi: 10.24191/jmeche.v20i3.23908.

[22] A. Raczkowski, Z. Suchorab, and P. Brzyski, "Computational fluid dynamics simulation of thermal comfort in naturally ventilated room," *MATEC Web Conf.*, vol. 252, p. 04007, 2019, doi: 10.1051/matecconf/201925204007.

[23] H. Qiao, X. Han, S. Nabi, and C. R. Laughman, "Coupled Simulation of a Room Air-conditioner with CFD Models for Indoor Environment," in *Modelica*, Mar. 2019, pp. 157–028.

[24] R. Widiastuti, M. I. Hasan, C. N. Bramiana, and P. U. Pramesti, "CFD Simulation on the Natural Ventilation and Building Thermal Performance," in *IOP Conf. Ser.: Earth Environ. Sci.*, Institute of Physics Publishing, Apr. 2020, doi: 10.1088/1755-1315/448/1/012004.